

System for lifetime measurements of alkali F-states with a diode-laser in the first step of a dipole-quadrupole excitation scheme

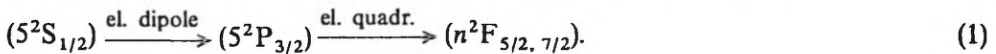
B. BIENIAK, K. FRONC, M. GLÓDŹ, J. SZONERT

Institute of Physics, Polish Academy of Sciences, al. Lotników 32/46, 02-668 Warszawa, Poland.

An experimental set-up is presented for lifetime measurements of F-states of alkali metal atoms. Its implementation is designed for rubidium. F-states were populated by stepwise dipole-quadrupole S-P-F transitions. Two components of the set-up, specially developed for experiment, are described in more detail. These are: (i) a stabilized diode-laser, and (ii) a general purpose PC-based system for on-line data acquisition and control of various experimental parameters. The set-up is adaptable to serve for other lifetime measurements.

1. Introduction — excitation/detection scheme

Different excitation/detection schemes were used in the lifetime measurements of alkali atom F-states, reported so far [1]–[5]. Usually, combinations of electric-dipole allowed transitions were applied to excite at first an appropriate D-level, and then another electric-dipole allowed (spontaneous or induced) transition was used to populate the F-level of interest (Fig. 1a–d). For example, a microwave induced nD - nF mixing was applied for Na atoms while superradiant (SR) transition from the higher excited D state to a F state for Rb and Cs atoms. SR was also used to populate an intermediate D state, both for Rb and Cs. In the present experiment, we applied an alternative scheme (Fig. 1e). A direct excitation of n^2F ($n = 6, 7, 8$) states of rubidium was accomplished by a two-step process: an electric-dipole allowed transition followed by an electric-quadrupole allowed one



The time-resolved fluorescence signal



was observed. Although an efficient excitation/detection system was necessary due to a low probability of the quadrupole transition, such a direct excitation scheme has clear advantages, *e.g.*, (i) the scheme does not rely on SR cascading with its specific requirements on working range of excited atoms density [2], [4], [5], (ii) except for accidental coincidence, in such a scheme it is not expected for detected wavelength to have a value close to that of an exciting wavelength, (iii) experimental results of level decay kinetics have direct physical interpretation.

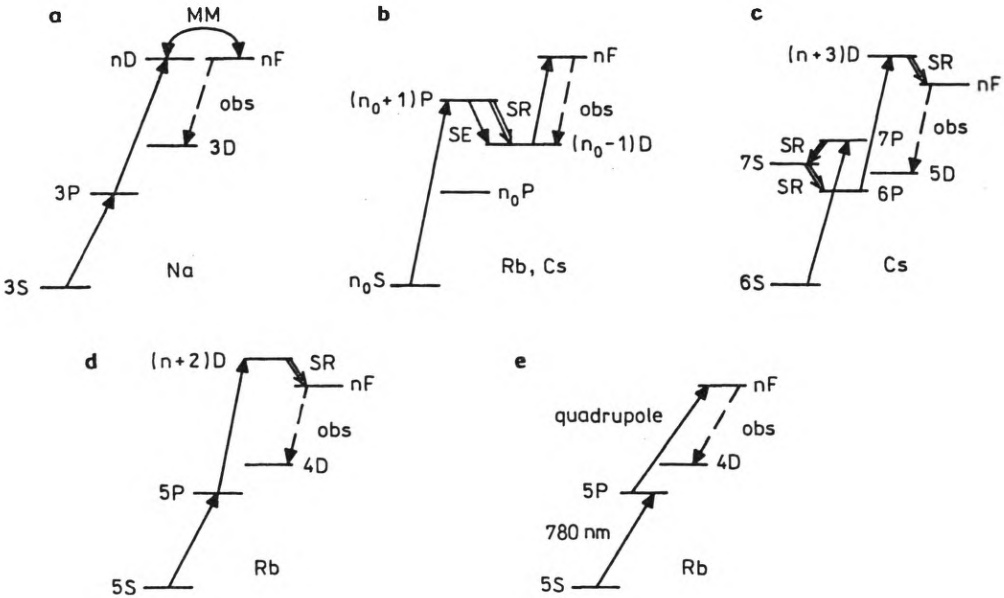


Fig. 1. Excitation/detection schemes used previously in lifetime measurements of the nF states of alkali atoms, symbols of the investigated elements are given (a–d) References: a – [1], b – for Rb (SR) [2], for Cs (SE) [3], for Cs (SR) [4], c – [4], d – [5]. Scheme based on two-step electric-dipole/electric-quadrupole transition applied in the present experiment (e). (Abbreviations: obs – observed fluorescence, SR – superradiance, SE – spontaneous emission, MM – microwave mixing)

In our experiment, a single mode c.w. semiconductor laser was used in the first step and a pulsed dye laser, in the second one. The detection path comprised a single photon counting system. In the following sections, a description of the experimental arrangement will be given. Two components, which were developed specially for this work, will be discussed in more detail: (i) the laser-diode system, and (ii) the PC-based system for data acquisition and parameters control.

2. Experimental arrangement

2.1. Description of the set-up

Figure 2 shows a scheme of the experimental set-up. A cylindrical cell (4 cm diameter, 11 cm length) made of Pyrex-glass, containing pure rubidium (ca. 98% of ^{87}Rb in an enriched isotopic mixture) without buffer gas, was placed in a two-chamber oven resistively heated by two temperature controllers. The cell was baked and evacuated to 10^{-8} Torr during 2 weeks before it was charged with a droplet of rubidium. The temperature of the cell was continuously monitored by five Ni-NiCr thermocouples fixed at different positions to the outer surface of the cell. The reference temperature with stability better than 0.1 K was delivered by

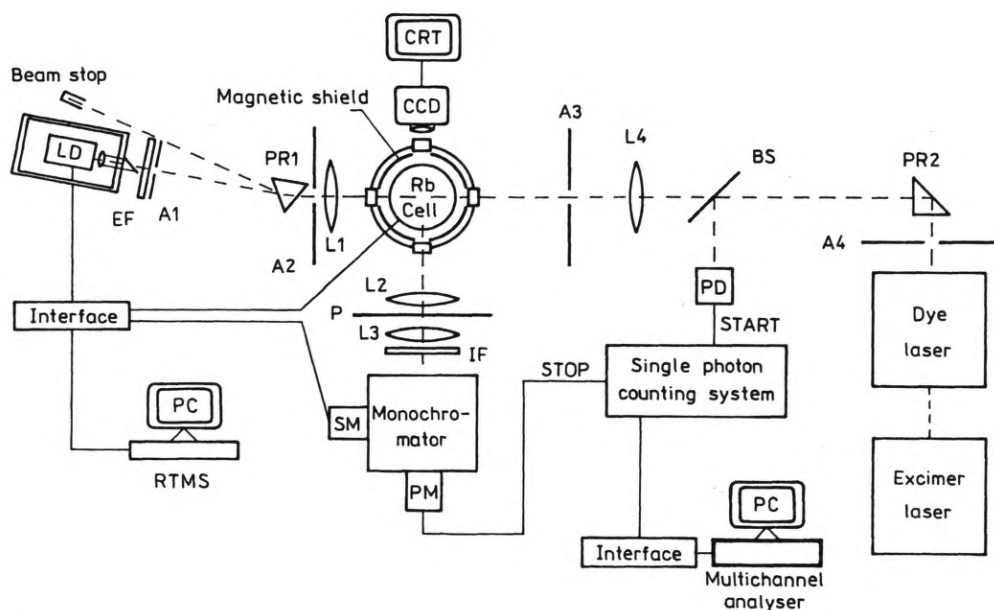


Fig. 2. Schematic diagram of lifetime measurement apparatus. Abbreviations: LD – laser diode, EF – coloured glass edge filter, A1–A4 – apertures, PR1 and PR2 – prisms, L1–L4 – lenses, P – linear polarizer, IF – interference filter, SM – step motor, PM – photomultiplier, PD – photodiode, BS – beam splitter

an ice-cell (type 16/120, IMP, modified). To avoid condensation of the Rb vapour onto the cell walls within the excitation region in the upper part of the cell, this part was maintained warmer. The temperature difference between the upper and the lower parts of the cell was kept at 4–6 K level. Longterm (*ca* 5 h) temperature stability of the cell was better than 0.2 K and 0.1 K at thermocouple position in the upper and in the lower parts, respectively. Cell temperature was kept in the 320–365 K range corresponding to an atomic number density of $N = (0.08 - 3) \times 10^{12} \text{ cm}^{-3}$. The influence of the earth's as well as stray magnetic fields was minimized with a two-fold magnetic shield surrounding the cell. In the first step of the excitation scheme (1) (and Fig. 1e), a c.w. single mode GaAlAs laser diode was used, tuned to the resonant transition at 780 nm (see Sect. 2.2 for more details). In the second step, an excimer laser pumped dye laser (Lumonics HD-500 pumped by EX-520) was applied. The dye laser tuned to 561, 537 or 522 nm, depending on the n^2F state excited, produced pulses of *ca* 5 ns duration and of *ca* 0.1 cm^{-1} bandwidth, typical pulse energy was 1 mJ at the repetition rate of 90–110 Hz. Both (dye and diode) laser beams were linearly polarized in vertical plane and directed antiparallely through the upper part of the cell, across the cylinder. The dye laser beam was softly focused with a $f = 1.5 \text{ m}$ lens, whose focal point was *ca* 0.5 m behind the oven. The diode laser beam was focused into the cell by a $f = 10 \text{ cm}$ lens. A set of apertures was used to ensure colinearity of beams and to minimize the stray light. Emerging

fluorescence (2) at 887, 827 or 793 nm, depending on the investigated upper state, was collected at a right angle to the polarization plane of the laser beams and imaged onto the fully opened (1.5 mm, spectral width 6 nm FWHM) slit of a grating monochromator by a two-lens optical system. A linear polarizer set at a magic angle (54.7°) relative to the polarization direction of the incident laser beams was inserted into the optical detection path to avoid possible errors due to hyperfine structure quantum beats and/or collisional depolarization [6]–[8]. Preliminary wavelength discrimination of the signal was provided by interchangeable IF filter(s) (typical bandpass 10 nm FWHM). Signal from the cooled (at -20°C) photomultiplier (Hamamatsu R943-02) was fed to the system for single photon counting (SPC) in delayed coincidence. A pile-up inspector was incorporated into the system. PC-based multichannel analyzer (MCA) was interfaced via a pulsed ADC with the time-to-amplitude converter (TAC) of the SPC system. Data gathered in the MCA were stored onto the disk for further analysis.

Another PC was used to control several parameters of the experiment. Laser diode parameters (drive current, case temperature, emitted power) as well as temperature readouts from the oven's thermocouples were monitored on-line, stored onto the disk and displayed, in real-time, on the screen. Detailed description of the software is given in Sec. 2.3.

2.2. Laser diode system

Due to their favourable characteristics, such as, *e.g.*, tunability, narrow bandwidth, ease of modulation or low cost, semiconductor diode laser emitting in infrared (and also in visible) have found various applications in atomic and molecular physics (*e.g.*, [9]–[11]). Different wavelength stabilization systems and constructions of laser heads (aimed, *e.g.*, at narrowing the linewidth) were used [12]–[16]. The frequency of the laser radiation is determined by both laser temperature and injection current. For GaAlAs laser of the type used in our experiment, the typical frequency changes range from -20 to -30 GHz/ $^\circ\text{C}$ and from -3 to -7 GHz/mA for temperature and injection current changes, respectively. Therefore, efforts were made to ensure an adequate temperature stabilization by providing a temperature control and a good thermal insulation of the laser, as well as a stable current supply. The diode used (Sharp LT021MF0, maximum rated output 15 mW) was placed inside of a solid copper block ($14 \times 50 \times 40$ mm) which itself was fixed onto a water-cooled thermoelectric 20 W Peltier-cooler. The strongly divergent laser diode beam was collimated by a single, small plastic lens (of the type used for laser heads in the compact-disk players). The temperature sensor (LM335AD) was placed in the vicinity of the laser diode case inside of the copper block. The temperature of the laser (or actually of the copper block) was actively stabilized in a temperature control loop with a PID controller (type 3304, Willmer) modified in our laboratory. (The temperature control device was an improved version of the one presented in [17].) The temperature down to -10°C with a long term (2 hours) stability within 1–5 mK was reached (see Fig. 3a), depending on the stability of ambient temperature and of cooling water temperature. The injection current was supplied

from a high stability current source (type 656, UNIPAN), which can deliver up to 100 mA of d.c. current with a nominal drift of the order of $1 \mu\text{A}/\text{h}$. In order to protect the laser against surcharge (static electricity, switch-on/-off effects), slow-start circuit based on two transistors and spike protective filter were used in the electric circuitry (e.g., [12], [18]).

In Figure 3b, an absorption spectrum of ^{87}Rb vapour at room temperature, obtained at 4 mW power level with our laser diode, is shown, reflecting the hyperfine structure (hfs) of the ground state (hfs of the upper state is too small to be resolved here).

The overall frequency stability of the laser was estimated by tuning the laser to the centre of one ($F = 2$) of the hfs components of the absorption line and then registering the absorption signal as a function of time. In Figure 3c thus obtained frequency drift from the absorption peak *vs.* time is shown. We found a drift of

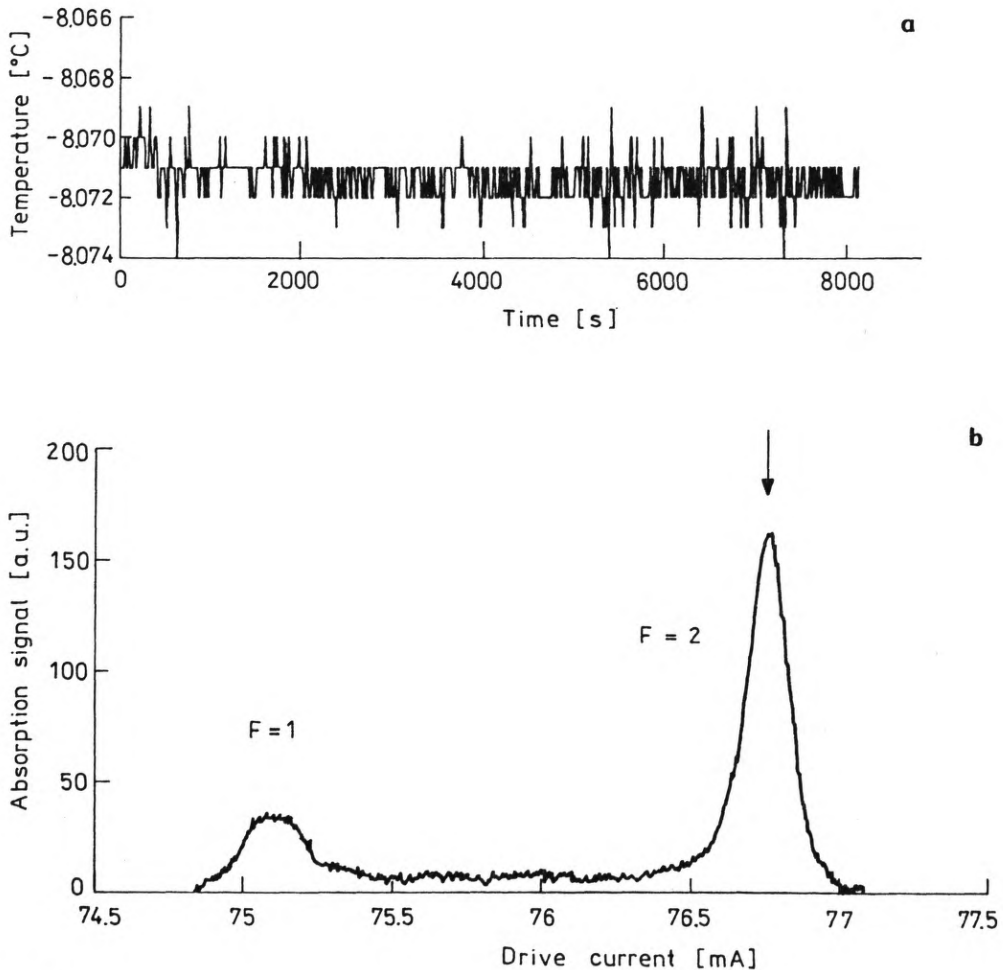


Fig. 3a, b

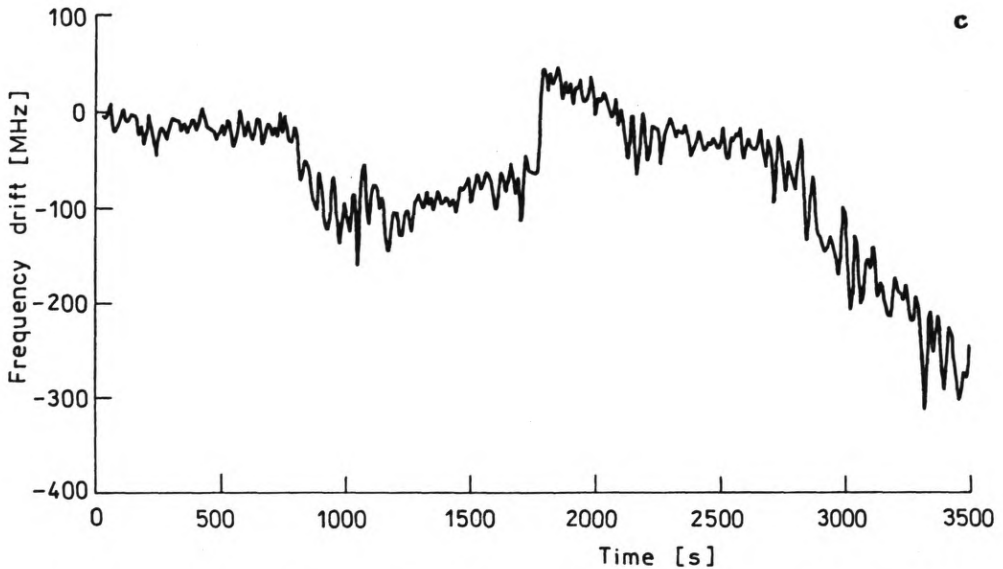


Fig. 3. Temperature stability of the laser head measured by the sensor placed close to the laser case (a). Absorption spectrum of ^{87}Rb vapour at the room temperature, obtained by tuning (the drive current of) the diode laser across the $5^2\text{S}_{1/2} - 5^2\text{P}_{3/2}$ resonance. Two components are due to hfs splitting of the ground state ($F = 1$ and $F = 2$ sublevels, distanced by 6.83 GHz). The $F = 2$ resonance was used in the excitation scheme of the experiment (b). Laser diode frequency drift (c)

300 MHz/h. It is a combined effect of the temperature/current instabilities and the noise introduced by slow-start circuitry which was constructed from low grade electronic components. The authors believe that with the use of low noise and thermally stable components the drift can be reduced by a factor of 5. In the course of the experiment, the laser line stability was visually monitored by means of CCD camera/CRT system which was directed to observe the laser diode induced resonance fluorescence. Stability checks and minor current adjustments were usually performed each 15–60 min to keep diode radiation wavelength in resonance with atomic transition. The achieved stability was quite satisfactory for the purpose of the present experiment.

2.3. On-line control of parameters of the experiment

The data-acquisition and handling system (RTMS – Real-Time Measurement System) was developed to serve the present experiment. However, its applicability is broader, since during many experiments a number of parameters has to be monitored. The program itself is prepared to run on PC under DOS operating system. This program is a skeleton which can service two types of requests:

1. Requests that have to be serviced at predetermined moments (called here timed-requests).
2. Requests that are handled in computer free time (called here free-time-requests).

Ad 1. Timed-requests — these are the ones effecting input of measurement results and output of control signals. During the program initialization process, first timed-requests to be serviced are placed into the timed-queue, with the indication of the instant of time when they have to be serviced. Time is determined with the accuracy to the interval between successive DOS interrupts 08H (timer) occurring 2^{16} times per hour, *ca* every 55 ms. While a request is being handled during DOS interrupt, the next request of the same kind (*e.g.*, the next request for readout of the same voltmeter) is placed in the timed-queue.

Ad 2. Free-time-requests — these are the requests for displaying the measured results or storing them to the disk file.

The software enables also on-line numerical analysis of the data (smoothing, averaging, *etc.*). Requests for such an analysis can belong to any of the above categories.

After the program is initialized, the main loop checks free-time-queue and handles its requests (Fig. 4a). Each occurrence of 08H interrupt suspends execution of the main loop and passes control to the routine servicing the queue of the timed-requests (Fig. 4b). After all requests from the timed-queue are executed, the control is passed back to the main program loop. The requests from the timed-queue have higher priority in the sense that they are executed at predetermined moments.

Various adjustable parameters are included in the parameters file. These parameters allow us:

1. To attach each of the data-collection (input) or experiment-control (output) channels to the appropriate device driver, thus determining the routine used for servicing the requests.

2. To choose the type of interface and, if necessary, also further links for communication with a given device (*e.g.*, COM2 or card 8255 and *i*-th IC on the card and port A of this IC).

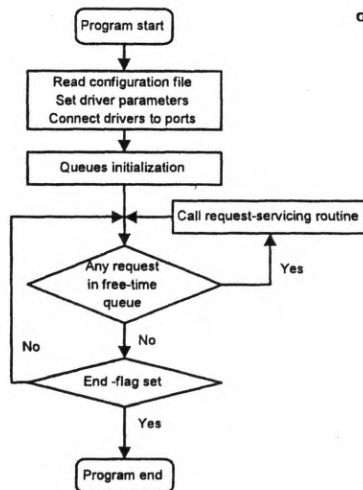


Fig. 4a

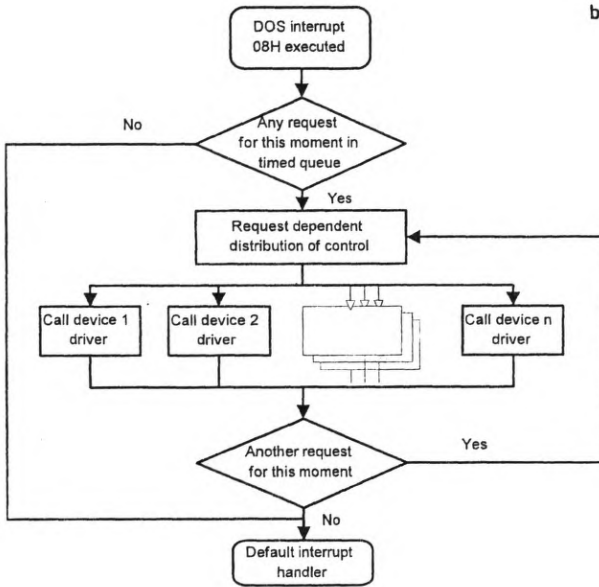


Fig. 4b

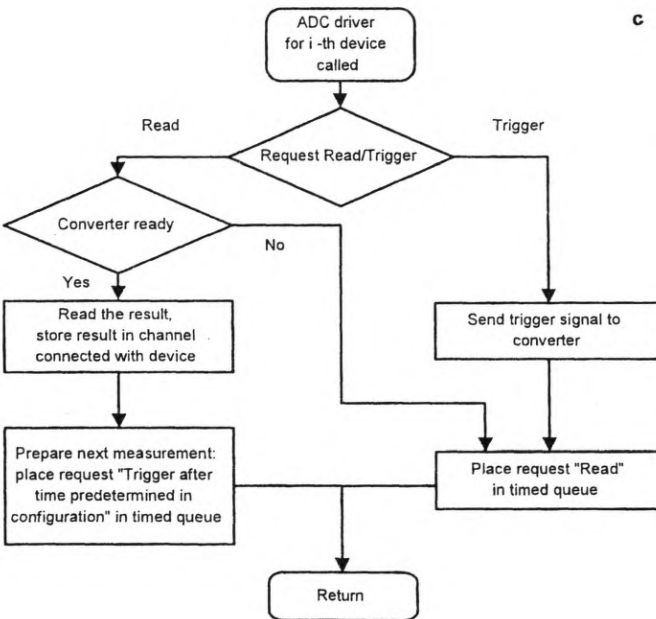


Fig. 4c

Fig. 4. Flow charts of different segments of the software discussed in Sec. 2.3. a – main loop of the program servicing the queue of the free-time-requests, b – routine servicing the queue of the timed-requests, executed each time 08H interrupt occurs, c – an example of a device driver for ADC

3. To link a certain input (data-collection) channel with a certain window on the display for plotting the results.

4. To determine other parameters, *e.g.*, frequency of readouts for ADC, parameters defining layout of display, *etc.*

The display parameters can be also changed on-line.

Software is written entirely in Turbo Pascal, programming language popular among physicists. This gives an opportunity to a user to write own procedures suited for particular devices used in the experiment.

In Figure 4c, a flow chart of an exemplary device driver for ADC is shown.

Hardware used in the present application of RTMS was based on several ADCs, on 8255 ICs and on a step motor attached to the tuning mechanism of the monochromator.

2.3.1. Simple example of application of RTMS

As an example, let us consider an experiment consisting in detection of a fluorescence spectrum. With the help of an ADC, a voltage signal proportional to the fluorescence intensity is registered. After each readout, monochromator selected wavelength is advanced by one step. During the initialization process the requests to trigger the ADC and to advance the monochromator tuning mechanism after a time interval required for completing the readout of the ADC are placed into the timed-queue. First request to be serviced is "Trigger" the ADC'. During this procedure, "Read" the result' request is placed into the timed-queue. While the result is being read, the successive request "Trigger" the ADC' is put into this queue, with indication of the time delay predetermined in the parameter file. At the same time the obtained number (fluorescence intensity) is sent to the measurement channel and request for updating the display is placed into the free-time-queue. The cycle of requests for advancing the monochromator is performed in a similar manner. It is possible to complement the converter driver with the request to repeat measurements until the readout is stabilized (if the converter has exponential characteristics of reaching the stable value), or with the request of averaging several readouts before the result is placed into the channel. User can also combine both channels: converter readouts and advancing the monochromator into a group in order to have all requests well synchronized.

3. Conclusions

The apparatus presented in this paper was built to measure lifetimes of the states with higher ($L=3$) orbital angular momentum, of the alkali metal atoms, with emphasis on Rb atoms. However, it can be also modified for other lifetime studies (see *e.g.*, [19]).

To excite Rb atoms from the ground 5S state to the nF ($n=6, 7, 8$) states, the stepwise excitation with electric-dipole allowed and electric-quadrupole allowed transitions was used. This scheme offers an efficient and direct method to excite the

states of interest and compares favourably with other schemes for population of the F states of alkali atoms, used in earlier lifetime studies.

The c.w. single mode diode laser emitting at 780 nm served to excite resonant 5S–5P transition in Rb vapour (first step in the excitation scheme). An adequate frequency stability of the laser was achieved in two steps: by the injection current control (the use of a high stability current supply) and by the stabilization of the laser case temperature (the use of a PID controller and thermal insulation). Since laser diodes emitting in other regions of near IR and in visible are also available (at relatively low cost), it is possible to adapt this system for efficient pumping of other atomic transitions by replacing the laser diode.

To assist the experiment, in which a number of parameters have to be controlled on-line, the PC based real-time measurement system (RTMS) was developed. Its software is entirely written in Turbo Pascal. With RTMS, analog signals can be repetitively digitized, stored and displayed on the screen. The system enables also sending control signals to the laboratory devices. The system is open for customizing, *i.e.*, adding to it user's own measurement-control procedures or drivers for laboratory specific devices.

The lifetime results, which are obtained with the above presented apparatus, will be presented elsewhere [20].

Acknowledgements – Authors thank L. Cyruliński and W. Samplawski for their expert technical assistance. This work was partly supported by the Committee for Scientific Research under grant No. 223419203.

References

- [1] GALLAGHER T. F., COOKE W. E., EDELSTEIN S. A., *Phys. Rev. A* **17** (1978), 904.
- [2] MAREK J., MÜNSTER P., *J. Phys. B* **13** (1980), 1731.
- [3] LUNDBERG H., SVANBERG S., *Z. Phys. A* **290** (1979), 127.
- [4] MAREK J., RYSCHKA M., *Phys. Lett. A* **74** (1979), 51.
- [5] HUGON M., GOUNAND F., FOURNIER P. R., *J. Phys. B* **11** (1978), L605.
- [6] PENDRILL L. R., SERIES G. W., *J. Phys. B* **11** (1978), 4049.
- [7] HANNAFORD P., LOWE R. M., *Aust. J. Phys.* **39** (1986), 829.
- [8] SCHADE W., WOLEJKO L., HELBIG V., *Phys. Rev. A* **47** (1993), 2099.
- [9] OHTSU M., TAKO T., [In] *Progress in Optics*, Vol. XXV, [Ed.] E. Wolf, Elsevier, Amsterdam 1988, p. 191.
- [10] WIEMAN C. E., HOLLBERG L., *Rev. Sci. Instrum.* **62** (1991), 1.
- [11] WITTEGREFE F., HOOPERLAND M. D., WOERDMAN J. P., *Meas. Sci. Technol.* **2** (1991), 304.
- [12] BRADLEY C. C., CHEN J., HULET R. G., *Rev. Sci. Instrum.* **61** (1990), 2097.
- [13] SAUNDERS P., KANE D. M., *Rev. Sci. Instrum.* **63** (1992), 2141.
- [14] LUDVIGSEN H., HOLMLUND C., *Rev. Sci. Instrum.* **63** (1992), 2135.
- [15] BARWOOD G. P., GILL P., ROWLEY W. R. C., *J. Mod. Optics* **37** (1990), 749.
- [16] MACADAM K. B., STEINBACH A., WIEMAN C., *Am. J. Phys.* **60** (1992), 1098.
- [17] SUCHENEK M., Diploma (in Polish), Military University of Technology, Warsaw 1992.
- [18] *Laser Diode User's Manual*, Sharp Corporation, 1988.
- [19] BIENIAK B., GŁÓDŹ M., GRZEGORZEWSKI P., SZONERT J., *Acta Phys. Pol. A* **85** (1994), 813.
- [20] SZONERT J., BIENIAK B., GŁÓDŹ M., PIECHOTA M., *Z. Phys. D* **33** (1995), in print.

Received September 19, 1994